 https://doi.org/10.3311/PPch.43504

Periodica Polytechnica Chemical Engineering, 70(2), pp. 208–214, 2026

Synthesis and Anticancer Effect of a Vindoline-Based Bis-Alkylated Resorcinol Derivative

Mónika Halmai[1], Nóra Nagy[1], Szabolcs Mayer[1], Péter Keglevich[1*], László Hazai[1*]

[1] Department of Organic Chemistry and Technology, Faculty of Chemical Technology and Biotechnology, Budapest University of Technology and Economics, Műegyetem rkp. 3, H-1111 Budapest, Hungary
[*] Corresponding authors, e-mail: keglevich.peter@vbk.bme.hu, hazai.laszlo@vbk.bme.hu

Received: 02 February 2026, Accepted: 27 April 2026, Published online: 02 June 2026

Abstract

Alkylation of the simple polyphenol model resorcinol with 10-chloroacetamidovindoline resulted in the corresponding O,O-disubstituted derivative containing two elements of the Vinca alkaloid. The in vitro anticancer activity of the hybrid was investigated on the NCI-60 human tumor cell line panel, and the most important value was obtained on UO-31 renal cancer cells (50% growth inhibition GI_{50} = 0.893 μM).

Keywords

resorcinol, vindoline, hybrid, anticancer effect

1 Introduction

The versatile chemical properties of resorcinol (**1**) allow it to be used in a wide range of industries. Its two hydroxyl groups, aromatic ring, and reactive meta-positions make it indispensable in the pharmaceutical, cosmetic, polymer production, dye, and analytical chemistry industries [1–4]. In terms of its biological effects, resorcinol is one of the oldest active ingredients applied in dermatology. It is used to treat a number of skin diseases due to its antiseptic, keratolytic, and antifungal properties. More importantly, however, its use as a building block for the preparation of anticancer derivatives containing, first of all, different heterocycles [5–11].

Nevertheless, resorcinol (**1**) is the structural unit of the skeleton of important antioxidant compounds (Fig. 1) such as resveratrol (**2**) or flavones, including one of the best-known derivatives, chrysin (**3**).

On the other hand, several representatives of the *Vinca* alkaloids (Fig. 2), such as vinblastine (**6**) and vincristine (**7**), are used in anticancer therapy [12–20]. These dimeric alkaloids consist of two monomers, vindoline (**4**)

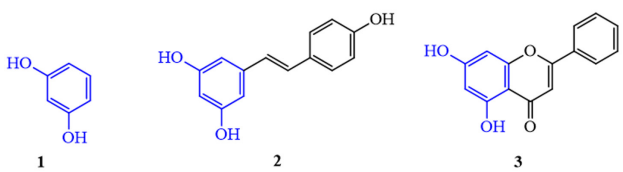

Fig. 1 Resorcinol (**1**) and its natural analogues: resveratrol (**2**) and chrysin (**3**)

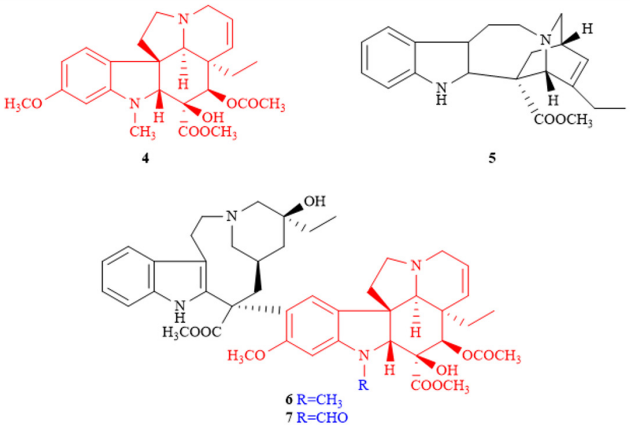

Fig. 2 Anticancer *Vinca* alkaloid dimers (**6** and **7**) and their monomers: vindoline (**4**) and catharanthine (**5**)

and catharanthine (**5**). In addition, several derivatives and hybrids of vindoline (**4**), which are inactive on their own, are known as efficient anticancer molecules [21–31].

Based on these data, it seemed worthwhile to investigate the possibility of coupling vindoline (**4**), the major alkaloid of *Catharanthus roseus*, with resorcinol (**1**) to identify potential new applications of vindoline and evaluate the anticancer activity of the resulting derivative.

2 Results and discussion

2.1 Chemistry

The coupling between resorcinol (**1**) and vindoline (**4**) was achieved via the O-alkylation of resorcinol (**1**) with

Cite this article as: Halmai, M., Nagy, N., Mayer, S., Keglevich, P., Hazai, L. "Synthesis and Anticancer Effect of a Vindoline-Based Bis-Alkylated Resorcinol Derivative", Periodica Polytechnica Chemical Engineering, 70(2), pp. 208–214, 2026. https://doi.org/10.3311/PPch.43504

10-chloroacetamidovindoline (**9**). The latter is a previously described intermediate designed for the synthesis of vindoline hybrids [24].

First, vindoline (**1**) underwent nitrosation at the active C-10 position, followed by reduction with NaBH4 to afford 10-aminovindoline (**8**) [25]. Subsequently, the 8 compound was N-acylated with chloroacetyl chloride. Finally, 10-chloroacetamidovindoline (**9**) was reacted with resorcinol (**1**) in acetonitrile in the presence of cesium carbonate and a catalytic amount of potassium iodide (Scheme 1). The reaction was initiated at room temperature, then the temperature was raised to 50 °C to increase the low conversion. After workup and purification by preparative thin-layer chromatography (TLC), structural analysis (NMR), high-resolution mass spectrometry (HRMS) revealed the formation of the desired bisalkylated hybrid (**10**), which was isolated in 38% yield.

2.2 Evaluation of the biological activities

The in vitro antiproliferative activities of vindoline (**4**) and the newly synthesized compound (**10**) were evaluated on a panel of 60 human tumor cell lines (NCI-60), comprising leukemia, non-small cell lung, colon, central nervous system (CNS), ovarian, renal, prostate, and breast cancers, as well as melanoma. The experiments were performed at the National Cancer Institute (NCI, USA) in accordance with standard screening protocols [32–37].

The screening data are summarized in Table 1, where cytotoxic effects were determined at a single concentration of 10 μM. The reported growth percentages reflect the proportion of viable tumor cells relative to untreated controls, while negative values indicate a pronounced reduction in cell number. For example, a value of 100 means no growth inhibition. A value of 25 would mean 75% growth inhibition. A value of 0 means no net growth over the course of the experiment. A value of −25 would mean 25% lethality. A value of −100 means all cells are dead. In line with previous findings, vindoline (**4**) displayed only marginal antiproliferative activity across the majority of tested cell lines. In contrast, the new hybrid (**10**) exhibited a markedly enhanced and broad-spectrum antiproliferative effect in the NCI-60 panel, demonstrating substantial growth inhibition in multiple tumor types.

Since compound 10 showed significant antiproliferative activity on several tumor cell lines during the one-dose test, it was subjected to a five-dose screening. The 50% growth inhibition (GI_{50}) and their mean values are given in Table 2. Based on the results, hybrid (**10**) exhibited an uniform antiproliferative effect in the low micromolar range across the entire NCI-60 panel. The mean GI_{50}

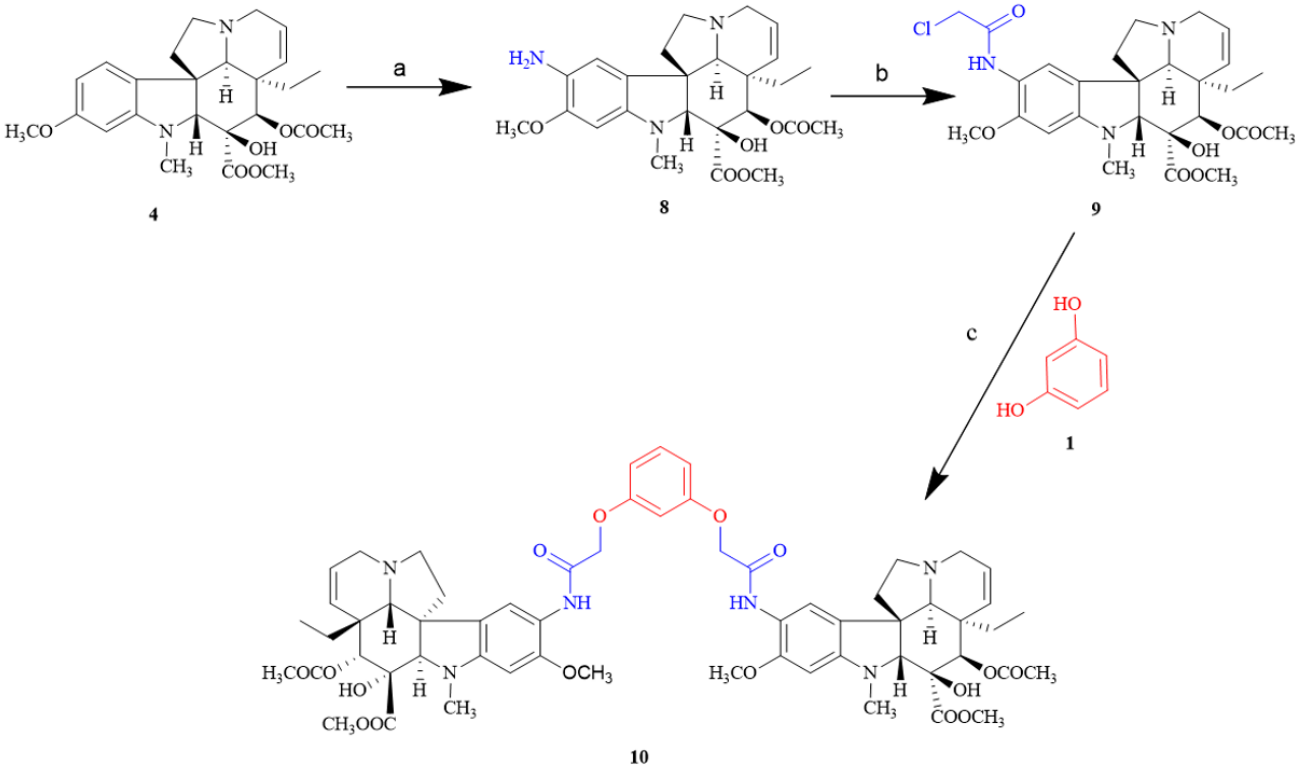

Scheme 1 Synthesis of hybrid **10**: (a) (1) THF, 1M HCl, $NaNO_2$, 0 °C, 30 min; (**2**) $NaBH_4$, MeOH, Ar, room temperature, 92%, (b) chloroacetyl chloride, abs. DCM, K_2CO_3, Ar, room temperature, 7 h, 64%; (c) Cs_2CO_3, KI, CH_3CN, 50 °C, 18 h, 38%.

Table 1 Growth percent rates of vindoline (**4**), and compound **10** at the concentration of 10 μM against 60 human cancer cell lines *in vitro*. All data with greater than 50% loss of cells are highlighted in bold.

Panel	Cell line	**4**	**10**
Leukemia	CCRF-CEM	96.54	14.92
	HL-60(TB)	103.96	0.53
	K-562	103.40	7.24
	MOLT-4	103.19	11.93
	RPMI-8226	100.94	−6.77
	SR	n.d.	5.63
Non-small cell lung cancer	A549/ATCC	93.52	−27.20
	EKVX	101.77	−44.99
	HOP-62	92.23	−42.83
	HOP-92	84.21	n.d.
	NCI-H226	104.40	−47.47
	NCI-H23	103.04	**−94.42**
	NCI-H322M	97.79	**−72.63**
	NCI-H460	104.23	1.11
	NCI-H522	88.55	**−74.92**
Colon cancer	COLO 205	n.d.	**−72.60**
	HCC-2998	117.70	**−95.69**
	HCT-116	104.47	−22.86
	HCT-15	99.02	−48.46
	HT29	98.55	**−69.79**
	KM12	102.15	**−96.71**
	SW-620	103.73	**−55.58**
CNS cancer	SF-268	99.98	10.51
	SF-295	99.51	**−79.27**
	SF-539	103.67	**−78.87**
	SNB-19	96.60	−39.72
	SNB-75	73.08	−2.00
	U251	99.44	−25.35
Melanoma	LOX IMVI	99.36	**−95.20**
	MALME-3M	97.96	**−75.70**
	M14	103.84	**−57.20**
	MDA-MB-435	105.29	**−76.33**
	SK-MEL-2	106.74	**−60.01**
	SK-MEL-28	105.79	52.96
	SK-MEL-5	102.00	**−99.00**
	UACC-257	98.69	**−61.26**
	UACC-62	94.73	**−91.08**
Ovarian cancer	IGROV1	98.42	−36.24
	OVCAR-3	112.39	**−91.10**
	OVCAR-4	98.82	−6.48
	OVCAR-5	91.21	**−55.13**
	OVCAR-8	99.84	−32.95
	NCI/ADR-RES	110.49	28.86
	SK-OV-3	107.57	**−65.19**
Renal cancer	786-0	104.33	1.47
	A498	99.59	**−86.06**
	ACHN	101.46	4.28
	CAKI-1	97.50	−46.15
	RXF 393	103.81	**−94.59**
	SN12C	96.08	**−82.73**
	TK-10	92.13	−29.79
	UO-31	83.93	**−78.13**
Prostate cancer	PC-3	88.31	n.d.
	DU-145	107.34	−23.58
Breast cancer	MCF7	99.03	**−56.59**
	MDA-MB-231/ATCC	97.65	**−92.82**
	HS 578T	113.32	−15.85
	BT-549	114.27	**−68.27**
	T-47D	95.68	−26.59
	MDA-MB-468	101.69	**−69.07**
Mean		100.08	−47.20

Note: n.d. means not determined.

Table 2 GI_{50} values (μM) of compound **10** against 60 human cancer cell lines *in vitro*. Values where GI_{50} < 1.0 μM are highlighted in bold. n.d. means not determined

Panel	Cell line	**10**	
		GI_{50}	Mean
Leukemia	CCRF-CEM	1.86	1.60
	HL-60(TB)	1.48	
	K-562	1.84	
	MOLT-4	1.52	
	RPMI-8226	1.25	
	SR	1.63	
Non-small cell lung cancer	A549/ATCC	1.51	1.18
	EKVX	1.33	
	HOP-62	1.09	
	HOP-92	**0.968**	
	NCI-H226	1.15	
	NCI-H23	1.12	
	NCI-H322M	1.25	
	NCI-H460	1.12	
	NCI-H522	1.17	
Colon cancer	COLO 205	1.18	1.16
	HCC-2998	1.13	
	HCT-116	1.33	
	HCT-15	1.22	
	HT29	1.12	
	KM12	1.09	
	SW-620	1.06	

Table 2 GI_{50} values (μM) of compound **10** against 60 human cancer cell lines *in vitro*. Values where GI_{50} < 1.0 μM are highlighted in bold. (continued)

Panel	Cell line	10	
		GI_{50}	Mean
CNS cancer	SF-268	**1.31**	1.27
	SF-295	1.03	
	SF-539	1.16	
	SNB-19	1.97	
	SNB-75	**0.992**	
	U251	1.15	
Melanoma	LOX IMVI	1.03	1.20
	MALME-3M	0.991	
	M14	1.15	
	MDA-MB-435	1.13	
	SK-MEL-2	1.14	
	SK-MEL-28	1.66	
	SK-MEL-5	1.05	
	UACC-257	1.29	
	UACC-62	1.11	
Ovarian cancer	IGROV1	1.45	1.57
	OVCAR-3	1.13	
	OVCAR-4	1.28	
	OVCAR-5	1.29	
	OVCAR-8	1.22	
	NCI/ADR-RES	3.36	
	SK-OV-3	1.27	
Renal cancer	786-0	1.71	1.37
	A498	1.12	
	ACHN	2.20	
	CAKI-1	1.31	
	RXF 393	1.16	
	SN12C	1.17	
	TK-10	1.40	
	UO-31	**0.893**	
Prostate cancer	PC-3	1.18	1.35
	DU-145	1.51	
Breast cancer	MCF7	1.89	1.39
	MDA-MB231ATCC	**0.949**	
	HS 578T	1.66	
	BT-549	1.08	
	T-47D	1.35	
	MDA-MB-468	1.22	
Mean		1.33	

Note: n.d. means not determined.

value was 1.33 μM, which is consistent with and supports the broad-spectrum efficacy observed in the single-dose screening. Only moderate variations were observed among the different tumor types, indicating that compound 10 does not exert a cell line-specific effect but rather displays a general antiproliferative profile. Notably, the compound achieved submicromolar GI_{50} values in five cell lines. The most pronounced activity was observed in the UO-31 (renal cancer) cell line, with a GI_{50} value of 0.893 μM.

Overall, these results demonstrate that the investigated compound shows significant antiproliferative activity, supporting its potential suitability for further biological and mechanistic investigations.

3 Materials and methods

3.1 General

All chemicals were purchased from Sigma-Aldrich (Budapest, Hungary) and were used as received. Melting points were measured on a VEB Analytik Dresden PHMK-77/1328 apparatus (Dresden, Germany) and are uncorrected. IR spectra were recorded on Zeiss IR 75 and 80 instruments (Thornwood, NY, USA). NMR measurements were performed on a Bruker Avance III HDX 500 MHz NMR spectrometer equipped with a $^{1}H\{^{13}C/^{15}N\}$ 5 mm TCI CryoProbe (Bruker Corporation, Billerica, MA, USA). ^{1}H and ^{13}C chemical shifts are given on the delta scale as parts per million (ppm) relative to tetramethyl silane. One-dimensional ^{1}H, and ^{13}C spectra and two-dimensional ^{1}H–^{1}H COSY, ^{1}H–^{1}H NOESY, ^{1}H–^{13}C HSQC, and ^{1}H–^{13}C HMBC spectra were acquired using pulse sequences included in the standard spectrometer software package (Bruker TopSpin 3.5, Bruker Corporation). ESI-HRMS and MS-MS analyses were performed on a Thermo Velos Pro Orbitrap Elite (Thermo Fisher Scientific, Bremen, Germany) system. The ionization method was electrospray ionization (ESI), operated in positive ion mode. The protonated molecular ion peaks were fragmented by collision-induced dissociation (CID) at a normalized collision energy of 35–65%. For the CID experiment, helium was used as the collision gas. The samples were dissolved in methanol. EI-HRMS analyses were performed on a Thermo Q Exactive GC Orbitrap (Thermo Fisher Scientific, Bremen, Germany) system. The ionization method was electron ionization (EI) and operated in positive ion mode. Electron energy was 70 eV and the source temperature was set at 250 °C. Data acquisition and analysis were accomplished with Xcalibur software version 4.0 (Thermo Fisher Scientific). TLC was carried out using DC-Alufolien Kieselgel 60 F_{254} (Merck, Budapest, Hungary) plates. Preparative TLC analyses were performed on silica gel 60 $PF_{254+366}$ (Merck) glass plates.

3.2 Chemistry

3.2.1 Preparation of 10-chloroacetamidovindoline (9)

This compound was prepared according to the recently presented results of Mayer et al. [24]. ^{1}H NMR, melting point, and R_f data were in good agreement with the literature.

3.2.2 Reaction of 10-chloroacetamidovindoline (9) with resorcinol (1); preparation of 10

190 mg (0.347 mmol, 2.0 eq.) of 10-chloroacetamidovindoline (**9**) was dissolved in 8 mL of acetonitrile. 19 mg (0.173 mmol, 1.0 eq.) of resorcinol (**1**), 113 mg (0.347 mmol, 2.0 eq.) of cesium carbonate, and a catalytic amount of potassium iodide were added. The reaction mixture was stirred at room temperature for 2 h. The reaction was monitored using TLC. Starting vindoline derivative (**9**) remained in the reaction mixture, so the external temperature was raised to 50 °C, and the reaction was continued for 18 h. The mixture was evaporated during the work-up. The resulting brown solid was dissolved in 30 mL of dichloromethane and washed with 25 mL of distilled water and 10 mL of saturated NaCl solution. After phase separation, the aqueous phases were extracted with 10-10 mL of dichloromethane. The combined organic phase was dried over magnesium sulfate. The drying material was filtered off, and the solution was evaporated. The resulting solid was purified by thin-layer chromatography (eluent: DCM/MeOH = 10/1). Based on structural studies, the hybrid (**10**) is a bisalkylated derivative, which was obtained in 38% yield (75 mg). TLC: R_f (DCM/MeOH = 15/1) = 0.49. Mp: 168-169 °C. IR (KBr): 2879; 2182; 1738; 1528; 1222; 1039 cm^{-1}. ^{1}H NMR (Fig. 3): (499.9 MHz; DMSO-d_6) δ (ppm): 0.43 (6H; t; J = 7.2 Hz; H3-18, H3-18'); 0.95 (2H; dq; J = 7.3, 14.0 Hz; H_x-19, H_x-19'); 1.47 (2H; dq; J = 14.0, 7.3 Hz; H_y-19, H_y-19'); 1.94 (6H; s; C(17)-OCOCH$_3$, C(17')-OCOCH$_3$); 2.15-2.26 (4H; m; H2-6, H2-6'); 2.52-2.58 (2H; m; H_x-5, H_x-5'); 2.60 (6H; s; N(1)-CH$_3$, N(1')-CH$_3$); 2.62 (2H; s; H-21, H-21'); 2.82 (2H; br d; J = 16.2 Hz; H_x-3, H_x-3'); 3.25-3.32 (2H; m; H_y-5, H_y-5'); 3.41 (2H; dd; J = 16.6, 4,7 Hz; H_y-3, H_y-3'); 3.54 (2H; s; H-2, H-2'); 3.66 (6H; s; C(16)-COOCH$_3$, C(16')-COOCH$_3$); 3.82 (6H; s; C(11)-OCH$_3$, C(11')-OCH$_3$); 4.68 (4H; s; H2-2", H2-11"); 5.09 (2H; br d; J = 10.1 Hz; H-15, H-15'); 5.20 (2H; s; H-17, H-17'); 5.82 (2H; br dd, J = 10.1, 4.7 Hz; H-14, H-14'); 6.43 (2H; s; H-12, H-12'); 6.62-6.67 (2H; m; H-7", H-9"); 6.67-6.70 (1H; m; H-5"); 7.25 (1H; t; J = 8.2 Hz; H-8"); 7.69 (2H; s; H-9, H-9'); 8.78 (2H; s; C(16)-OH, C(16')-OH,); 9.02 (2H; s; C(10)-NH-C(1"), C(10')-NH-C(12")). 13C NMR: (125.7 MHz; DMSO-d_6) δ (ppm): 7.5 (C-18, C-18'); 20.6 (C(17)-OCOCH$_3$, C(17')-OCOCH$_3$,); 30.4 (C-19, C-19'); 38.6 (N(1)-CH$_3$, N(1')-CH$_3$); 42.4 (C-20, C-20'); 43.6 (C-6, C-6'); 50.3 (C-3, C-3'); 51.0 (C-5, C-5'); 51.6 (C(16)-COOCH$_3$, C(16')-COOCH$_3$) 52.4 (C-7, C-7'); 55.9 (C-(11)-OCH$_3$, C-(11')-OCH$_3$); 66.1 (C-21, C-21'); 67.0 (C-2", C-11"); 75.8 (C-17, C-17'); 78.6 (C-16, C-16'); 82.7 (C-2, C-2'); 93.9 (C-12, C-12'); 101.9 (C-5"); 107.7 (C-7", C-9"); 116.6 (C-9, C-9'); 118.2 (C-10, C-10'); 123.6 (C-8, C-8'); 124.4 (C-14, C-14'); 129.8 (C-15, C-15'); 130.1 (C-8"); 149.6 (C-13, C-13'); 150.9 (C-11, C-11'); 158.6 (C-4", C-6"); 165.5 (C-1", C-12"); 170.0 (C(17)-OCOCH$_3$, C(17')-OCOCH$_3$); 171.5 (C(16)-COOCH$_3$, C(16)-COOCH$_3$). HRMS: (M+2H)/2 = 567.25737 (delta = −0.3 ppm; $C_{60}H_{74}O_{16}N_6$). HR-ESI-MS-MS (CID = 40%; rel. int. %): 558(8); 537(100); 528(6); 507(18); 432(15); 403(5).

4 Conclusions

The synthesis of the bis-alkylated derivative obtained by the reaction of resorcinol and two moieties of vindoline was presented as an interesting example of a hybrid of a simple polyphenol model and a *Vinca* alkaloid. The anticancer activity of the obtained product was investigated on 60 human cancer cell lines. The new compound showed submicromolar antiproliferative effect against several tested cell lines, including HOP-92 non-small lung cancer, SNB-75 CNS cancer, MALME-3M melanoma, and MDA-MB-231/ATCC breast cancer cells. The most potent activity was observed toward UO-31 renal cancer cells, with a GI_{50} value of 0.893 μM.

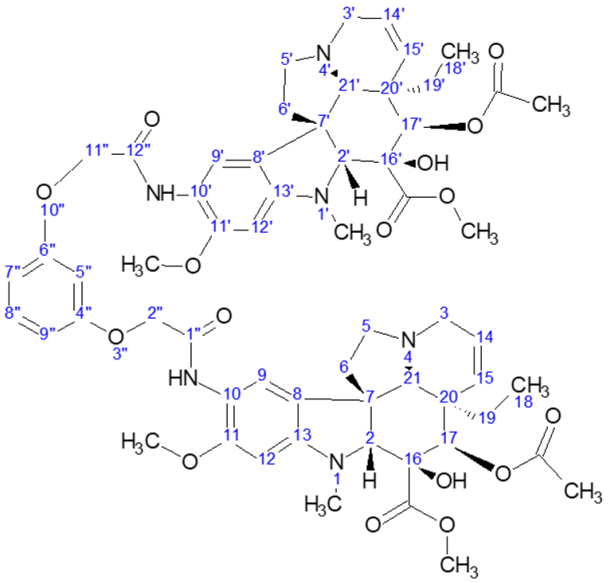

Fig. 3 The skeleton numbering of compound 10 used for NMR assignment

Acknowledgement

Project no. RRF-2.3.1-21-2022-00015 has been implemented with the support provided by the European Union (The National Research, Development and Innovation Office, PharmaLab, Széchenyi Plan Plus, National Laboratory Program). The project supported by the Doctoral Excellence Fellowship Programme (DCEP) is funded by the National Research Development and Innovation Fund of the Ministry of Culture and Innovation and the Budapest University of Technology and Economics. This work was also supported by the Servier Beregi Scholarship. The scientific work and results publicised in this article was reached with the sponsorship of Gedeon Richter Talentum Foundation in framework of Gedeon Richter Excellence PhD Scholarship of Gedeon Richter. We thank Áron Szigetvári, Márton Weber, Miklós Dékány and Csaba Szántay, Jr., Gedeon Richter Plc., for the NMR and MS measurements and interpretations.

References

[1] Durairaj, R. B. "Resorcinol: Chemistry, Technology and Applications", Springer: Berlin, Heidelberg, 2005. https://doi.org/10.1007/3-540-28090-1

[2] Badhe, Y., Balasubramanian, K. "Novel hybrid ablative composites of resorcinol formaldehyde as thermal protection systems for re-entry vehicles", RSC Advances, 4, pp. 28956–28963, 2014. https://doi.org/10.1039/C4RA03316G

[3] Nagy, B., Domán, A., Menyhárd, A., László, K. "Influence of Graphene Oxide Incorporation on Resorcinol-Formaldehyde Polymer and Carbon Aerogels", Periodica Polytechnica Chemical Engineering, 62(4), pp. 441–449, 2018. https://doi.org/10.3311/PPch.12915

[4] Matiz, C., Castellanos, K., Maldonado, M. "Resorcinarene-Based Polymer Conjugated for Pharmaceutical Applications", Processes, 13(5), 1325, 2025. https://doi.org/10.3390/pr13051325

[5] Li, Y., Dong, J., Quin, J.-J. "Small molecule inhibitors targeting heat shock protein 90: An updated review", European Journal of Medicinal Chemistry, 275, 116562, 2024. https://doi.org/10.1016/j.ejmech.2024.116562

[6] Beaumet, M., Lazinski, L. M., Maresca, M., Hudecoeur, R. "Tyrosinase Inhibition and Antimelanogenic Effects of Resorcinol-Containing Compounds", ChemMedChem, 19, e202400314, 2024. https://doi.org/10.1002/cmdc.202400314

[7] Matysiak, J., Karpińska, M. M., Skrzypek, A., Wietrzyk, J., Kłopotowska, D., Niewiadomy, A., Paw, B., Juszczak, M., Rzeski, W. "Design, Synthesis and Antiproliferative Activity against Human Cancer Cell Lines of Novel Benzo-, Benzofuro-, Azolo- and Thieno-1,3-Thiazinone Resorcinol Hybrids", Arabian Journal of Chemistry, 12(8), pp. 2655–2667, 2019. https://doi.org/10.1016/j.arabjc.2015.05.006

[8] Brizzi, A., Brizzi, V., Cascio, M. G., Corelli, F., Guida, ..., Di Marzo, V. "New Resorcinol-Anandamide 'Hybrids' as Potent Cannabinoid Receptor Ligands Endowed with Antinociceptive Activity in Vivo", Journal of Medicinal Chemistry, 52(8), pp. 2506–2514, 2009. https://doi.org/10.1021/jm8016255

[9] Nepali, K., Lin, M.-H., Chao, M.-W., Peng, S.-J., Hsu, K.-C., Lin, T. E., Chen, M.-C., Lai, M.-J., Pan, S.-L., Liou, J.-P. "Amide-tethered quinoline-resorcinol conjugates as a new class of HSP90 inhibitors suppressing the growth of prostate cancer cells", Bioorganic Chemistry, 91, 103119, 2019. https://doi.org/10.1016/j.bioorg.2019.103119

[10] Lynch, B. S., Delzell, E. S., Bechtel, D. H. "Toxicology review and risk assessment of resorcinol: Thyroid effects", Regulatory Toxicology and Pharmacology, 36(2), pp. 198–210, 2002. https://doi.org/10.1006/rtph.2002.1585

[11] Galindres, D. M., Cifuentes, D., Tinoco, L. E., Murillo-Acevedo, Y., Rodrigo, M. M., Ribeiro, A. C. F., Esteso, M. A. A "Review of the Application of Resorcinarenes and SBA-15 in Drug Delivery", Processes, 10(4), 684, 2022. https://doi.org/10.3390/pr10040684

[12] Keglevich, P., Hazai, L., Kalaus, G., Szántay, C. "Modifications on the Basic Skeletons of Vinblastine and Vincristine", Molecules, 17(5), pp. 5893–5914, 2012 https://doi.org/10.3390/molecules17055893

[13] Assunção, H. C., Silva, P. M. A., Bousbaa, H., Cidade, H. "Recent Advances in Microtubule Targeting Agents for Cancer Therapy", Molecules, 30(16), 3314, 2025. https://doi.org/10.3390/molecules30163314

[14] Verma, V., Sharma, S., Gaur, K., Kumar, N. "Role of vinca alkaloids and their derivatives in cancer therapy", World Journal of Advanced Research and Reviews, 16(3), pp. 794–800, 2022. https://doi.org/10.30574/wjarr.2022.16.3.1378

[15] Banyal, A., Tiwari, S., Sharma, A., Chanana, I., Patel, S. K. S., Kulshrestha, S., Kumar, P. "Vinca alkaloids as a potential cancer therapeutics: recent update and future challenges", 3 Biotech, 13(6), 211, 2023. https://doi.org/10.1007/s13205-023-03636-6

[16] Taub, J. W., Buck, S. A., Xavier, A. C., Edwards, H., Matherly, L. H., Ge, Y. "The evolution and history of Vinca alkaloids: From the Big Bang to the treatment of pediatric acute leukemia", Pediatric Blood & Cancer, 71(11), e31247, 2024. https://doi.org/10.1002/pbc.31247

[17] Ambardekar, S., Patil, S., Gurav, N., Mujawar, S. "Vinca Alkaloids in Cancer Therapy: Mechanisms, Biosynthesis, and Advances in Therapeutic Applications", International Journal of Scientific Research and Technology, 2(1), pp. 298–314, 2025. https://doi.org/10.5281/zenodo.14695718

[18] Keglevich, P., Zupkó, I., Szente, L., Puskás, I., Szigetvári, Áron, Mayer, S., Hazai, L. "Does Vinblastine Retain its Anticancer Effect in the Presence of Cyclodextrin? A Preliminary Study", Periodica Polytechnica Chemical Engineering, 68(2), pp. 133–139, 2024. https://doi.org/10.3311/PPch.23503

[19] Zhou, Q., Jin, M., Cui, Y., Jiang, S., Shang, P., Li, L. "Advances in pharmacological activity and drug delivery systems of vinca alkaloids", Natural Product Research, 2025. https://doi.org/10.1080/14786419.2025.2494625

[20] Sarkar, S., Sharma, S. "Therapeutic insights into Catharanthus roseus: Advances in vinca alkaloid production and cancer treatment", South African Journal of Botany, 184, pp. 780–793, 2025. https://doi.org/10.1016/j.sajb.2025.06.045

[21] Gherbovet, O., Sánchez-Murcia, P. A., Alvarez, M. C. G., Bignon, J., Thoret, S., Gagob, F., Roussi, F. "Synthesis and evaluation of hybrid molecules targeting the vinca domain of tubulin", Organic & Biomolecular Chemistry, 13(10), pp. 3144–3154, 2013. https://doi.org/10.1039/C4OB02114B

[22] Sammer, A. Y., Vendier, L., Massiot, G. "Structure and Synthesis of Vindolicine and Derivatives", Chemistry & Biodiversity, 21(4), e202301928, 2024. https://doi.org/10.1002/cbdv.202301928

[23] Ali, S., Hénon, E., Leroy, R., Massiot, G. "Addition of Vindoline to *p*-Benzoquinone: Regiochemistry, Stereochemistry and Symmetry Considerations", Molecules, 26(21), 6395, 2021. https://doi.org/10.3390/molecules26216395

[24] Mayer, S., Nagy, N., Keglevich, P., Szigetvári, Á., Dékány, M., Szántay, C., Jr., Hazai, L. "Synthesis of Novel Vindoline-Chrysin Hybrids", Chemistry & Biodiversity, 19(1), e202100725, 2021. https://doi.org/10.1002/cbdv.202100725

[25] Zsoldos, B., Nagy, N., Donkó-Tóth, V., Keglevich, P., Weber, M., Dékány, M., Nehr-Majoros, A., Szőke, É., Helyes, Z., Hazai, L. "Novel Piperazine Derivatives of Vindoline as Anticancer Agents", International Journal of Molecular Sciences, 25(14), 7929, 2024. https://doi.org/10.3390/ijms25147929

[26] Keglevich, P., Hazai, L., Kalaus, G., Szántay, C. "Cyclopropanation of Some Alkaloids", Periodica Polytechnica Chemical Engineering, 59(1), pp. 3–15, 2015. https://doi.org/10.3311/PPch.7257

[27] Mayer, S., Keglevich, A., Sepsey Für, C., Bölcskei, H., Ilkei, V., Keglevich, P., Hazai, L. "Results in Chemistry of Natural Organic Compounds. Synthesis of New Anticancer Vinca Alkaloids and Flavone Alkaloids", Chemistry, 2(3), pp. 714–726, 2020. https://doi.org/10.3390/chemistry2030046

[28] Keglevich, A., Zsiros, V., Keglevich, P., Szigetvári, Á., Dékány, M., Szántay, C., Jr., Mernyák, E., Wölfling, J., Hazai, L. "Synthesis and *In Vitro* Antitumor Effect of New Vindoline-steroid Hybrids", Current Organic Chemistry, 23(8), pp. 959–967, 2019. https://doi.org/10.2174/1385272823666190614113218

[29] Keglevich, A., Szigetvári, Á., Dékány, M., Szántay Jr., C., Keglevich, P., Hazai, L. "Synthesis and *in vitro* Antitumor Effect of New Vindoline Derivatives Coupled with Triphenylphosphine", Current Organic Chemistry, 23(7), pp. 852–858, 2019. https://doi.org/10.2174/1385272823666190524083236

[30] Halmai, M., Donkó-Tóth, V., Keglevich, P., Kánai, K., Weber, M., ..., Hazai, L. "Synthesis and *In Vitro* Evaluation of the Anticancer Effect of Novel Phosphonium Vindoline Derivatives", International Journal of Molecular Sciences, 26(8), 3775, 2025. https://doi.org/10.3390/ijms26083775

[31] Mayer, S., Herr, D. M., Nagy, N., Donkó-Tóth, V., Keglevich, P., Weber, M., Dékány, M., Hazai, L. "Synthesis and *In Vitro* Anticancer Evaluation of Chrysin Containing Hybrids and Other Chrysin Derivatives", Periodica Polytechnica Chemical Engineering, 67(2), pp. 316–336, 2023. https://doi.org/10.3311/PPch.21919

[32] Monks, A., Scudiero, D., Skehan, P., Shoemaker, R. H., Paull, K., …, Boyd, M. "Feasibility of a high-flux anticancer drug screen using a diverse panel of cultured human tumor cell lines", Journal of the National Cancer Institute, 83(11), pp. 757–766, 1991. https://doi.org/10.1093/jnci/83.11.757

[33] Shoemaker, R. H. "The NCI60 human tumour cell line anticancer drug screen", Nature Reviews Cancer, 6(10), pp. 813–823, 2006. https://doi.org/10.1038/nrc1951

[34] Alley, M. C., Scudiero, D. A., Monks, A. M. Hursey, L., Czerwinski, M. J., Fine, D. L., Abbott, B. J., Mayo, J. G., Shoemaker, R. H., Boyd, M. R. "Feasibility of Drug Screening with Panels of Human Tumor Cell Lines Using a Microculture Tetrazolium Assay", Cancer Research, 48(3), pp. 589–601, 1988.

[35] Shoemaker, R. H., Monks, A., Alley, M. C., Scudiero, D. A., Fine, D. L., McLemore, T. L., Abbott, B. J., Paull, K. D., Mayo, J. G., Boyd, M. R. "Development of Human Tumor Cell Line Panels for Use in Disease-Oriented Drug Screening", Progress in Clinical and Biological Research, 276, pp. 265–286, 1988.

[36] Skehan, P., Storeng, R., Scudiero, D., Monks, A., McMahon, J., Vistica, D., Warren, J. T., Bokesh, H., Kennedy, S., Boyd, M. R. "New Colorimetric Cytotoxicity Assay for Anticancer-Drug Screening", Journal of the National Cancer Institute, 82(13), pp. 1107–1112, 1990. https://doi.org/10.1093/jnci/82.13.1107

[37] National Cancer Institute "NCI-60 Screening Methodology", National Cancer Institute, U.S. Department of Health & Human Services Rockville, MD, USA, 2025. Available at: https://dctd.cancer.gov/drug-discovery-development/assays/high-throughput-screening-services/nci60/submitting-compounds/screening-methodology.pdf (Accessed: 28 January 2026)